

6DoF SLAM aided GNSS/INS Navigation in GNSS Denied and Unknown Environments

Jonghyuk Kim and Salah Sukkarieh¹

Department of Engineering, The Australian National University, ACT200, Australia
e-mail: jonghyuk.kim@anu.edu.au Tel: +61 (0)2 6125 2462; Fax: +61 (0)2 6125 0506,

¹ARC Centre of Excellence for Autonomous Systems, The University of Sydney, Australia
e-mail: salah@acfr.usyd.edu.au Tel: +61 (0)2 9351 8515; Fax: +61 (0)2 9351 7474

Received: 6 December 2004 / Accepted: 12 July 2005

Abstract. This paper presents the results of augmenting 6DoF Simultaneous Localisation and Mapping (SLAM) with GNSS/INS navigation system. SLAM algorithm is a feature based terrain aided navigation system that has the capability for online map building, and simultaneously utilising the generated map to constrain the errors in the on-board Inertial Navigation System (INS). In this paper, indirect SLAM is developed based on error analysis and then is integrated to GNSS/INS fusion filter. If GNSS information is available, the system performs feature-based mapping using the GNSS/INS solution. If GNSS is not available, the previously and/or newly generated map is now used to estimate the INS errors. Simulation results will be presented which shows that the system can provide reliable and accurate navigation solutions in GNSS denied environments for an extended period of time.

Keywords: 6DoF SLAM, low cost GNSS/INS, vision sensor, features mapping, UAV

1 Introduction

The Global Navigation Satellite System (GNSS) is a space-borne, radio navigation system. In airborne navigation, its complementary characteristics to the Inertial Navigation System (INS) make it an excellent aiding system, resulting in integrated GNSS/INS navigation systems. In UAV application, due to its limited payload capacity and accurate navigation requirement to guide and control the vehicle, the low-cost, light-weighted, and compact-sized GNSS/INS system has been focused significantly.

The main drawback in the cost-effective GNSS/INS system is that the integrated system becomes more dependent on the availability and quality of GNSS information. Unfortunately, GNSS information can be easily blocked or jammed by intentional/unintentional interference. Even a short duration of satellite signal blockage can degrade the navigation solution significantly as shown in Kim 2004.

In this paper, a new concept of terrain-aided navigation, known as Simultaneous Localisation and Mapping (SLAM) is considered to aid INS during GNSS denied situations. SLAM was firstly addressed in the paper by Smith and Cheeseman, 1987 and has evolved from the robotics research community to explore unknown environments, where absolute information is not available (Dissanayake and *et al* 2001, Guivant 2001, Williams and *et al* 2001). Contrary to the exiting terrain aided navigation system, SLAM does not require any pre-surveyed map database. It builds the map incrementally by sensing environment and uses the map to localise the vehicle simultaneously, which results in a truly self-contained autonomous navigation system.

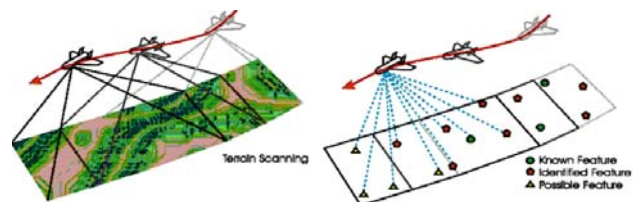


Fig. 1 The overall structure of SLAM is about building a relative map of feature using relative observations, defining a map, and using this map to localise the vehicle simultaneously.

The nonlinear 6DoF SLAM algorithm, incorporating IMU as its core dead-reckoning sensor, was firstly demonstrated in paper by Kim and Sukkarieh, 2004. Its airborne application is described in Figure 1. The vehicle

starts navigation from an unknown location and an unknown environment. The vehicle navigates by using its dead-reckoning sensor or vehicle model. As the onboard sensors detect features from the environment, the SLAM estimator augments the feature locations to a map in some global reference frame and begins to estimate the vehicle and map states together with successive observations. The ability to estimate both the vehicle location and the map is due to the statistical correlations that exist within the estimator between the vehicle and features, and between the features themselves. As the vehicle proceeds through the environment and re-observes old features, the map accuracy converges to a lower limit, which is a function of the initial vehicle uncertainty when the first feature was observed (Dissanayake and *et al*, 2001). In addition, the vehicle uncertainty is also constrained simultaneously.

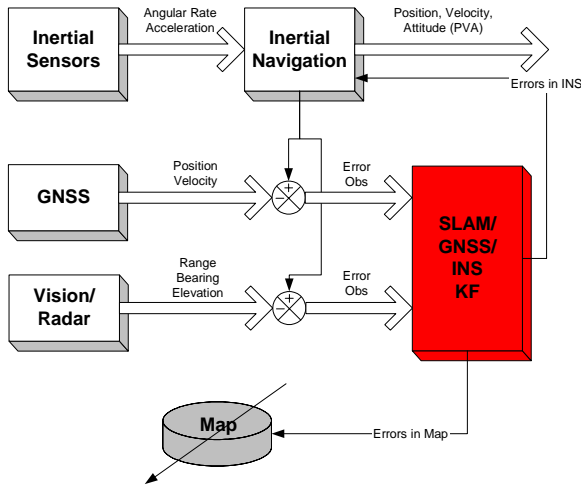


Fig. 2 The architecture of SLAM augmented GNSS/INS system

In this paper the 6DoF SLAM algorithm is augmented to the GNSS/INS navigation system to provide reliable INS aiding in GNSS denied environment. Figure 2 presents the architecture of the SLAM augmented GNSS/INS system. The key feature in this approach is the complementary fusion structure, which has high-speed INS module and low-speed and computationally expensive SLAM/GNSS/INS filter. To achieve this, the nonlinear SLAM algorithm was re-casted into linearised error state form as in the work of Kim, 2004, then it is augmented to fusion filter. In this architecture, the INS and map is maintained outside the SLAM filter and the map is treated as external map database. The fusion filter works as either feature-tracking filter or SLAM filter depending on the availability of GNSS observation. If GNSS provides reliable observations, then the on-board terrain observations are used to build the feature map and SLAM/GNSS/INS filter estimates the errors in INS and

map, which results in a feature (or target)-tracking system. However, in GNSS-denied situation, the terrain observations are solely used to estimate the errors in INS and map, which results in SLAM mode operation. Although there are no global observations from GNSS, the constant re-observation and revisit processes can improve the quality of map and navigation performance.

Section 2 will present the external INS loop and map and Section 3 will formulate the error model of SLAM/GNSS/INS algorithm and Kalman filter structure. In Section 4, simulation results are provided based on our Brumby UAV, then Section 5 will provide conclusions with future work.

2 External INS loop and map

In the complementary SLAM/GNSS/INS structure, the SLAM filter aids the external INS loop in a complementary fashion. The inertial navigation algorithm is to predict the high-dynamic vehicle states from the Inertial Measurement Unit (IMU) measurements. In this implementation a quaternion-based strapdown INS algorithm formulated in earth-fixed tangent frame is used (Kim, 2004):

$$\begin{bmatrix} \mathbf{p}^n(k) \\ \mathbf{v}^n(k) \\ \mathbf{q}^n(k) \end{bmatrix} = \begin{bmatrix} \mathbf{p}^n(k-1) + \mathbf{v}^n(k-1)\Delta t \\ \mathbf{v}^n(k-1) + [(\mathbf{q}^n(k-1) \otimes \mathbf{f}^b(k)) \otimes (\mathbf{q}^n)^*(k-1) + \mathbf{g}^n] \Delta t \\ \mathbf{q}^n(k-1) \otimes \Delta \mathbf{q}^n(k-1) \end{bmatrix} \quad (1)$$

where $\mathbf{p}^n(k)$, $\mathbf{v}^n(k)$, $\mathbf{q}^n(k)$ represent position, velocity, and quaternion respectively at discrete time k , Δt is the time for the position and velocity update interval, $(\mathbf{q}^n)^*(k)$ is a quaternion conjugate for the vector transformation, \otimes represents a quaternion multiplication, and $\Delta \mathbf{q}^n(k)$ is a delta quaternion computed from gyroscope readings during the attitude update interval.

3 Complementary SLAM/GNSS/INS Algorithms

The mathematical framework of the SLAM algorithm is based on an estimation process which, when given a kinematic/dynamic model of the vehicle and relative observations between the vehicle and features, estimates the structure of the map and the vehicle's position, velocity and orientation within that map. In this work, the Kalman Filter (KF) is used as the state estimator.

3.1 Augmented Error State

In complementary SLAM, the state is now defined as the error state of vehicle and map:

$$\delta \mathbf{x}(k) = [\delta \mathbf{x}_v(k), \delta \mathbf{x}_m(k)]^T \quad (2)$$

The error state of the vehicle $\delta \mathbf{x}_v(k)$ comprises the errors in the INS indicated position, velocity and attitude expressed in the navigation frame:

$$\delta \mathbf{x}_v(k) = [\delta \mathbf{p}^n(k), \delta \mathbf{v}^n(k), \delta \boldsymbol{\psi}^n(k)]^T \quad (3)$$

The error state of the map $\delta \mathbf{x}_m(k)$ also comprises the errors in 3D feature positions in the navigation frame. The size of state is also dynamically augmented with the new feature error after the initialisation process,

$$\delta \mathbf{x}_m(k) = [\delta \mathbf{m}_1^n(k), \delta \mathbf{m}_2^n(k), \dots, \delta \mathbf{m}_N^n(k)]^T, \quad (4)$$

where N is the current number of registered features in the filter and each state consists of a 3D position error.

3.2 SLAM Error Model

The linearised SLAM system in discrete time can be written as

$$\delta \mathbf{x}(k+1) = \mathbf{F}(k)\delta \mathbf{x}(k) + \mathbf{G}(k)\mathbf{w}(k) \quad (5)$$

where $\delta \mathbf{x}(k)$ is the error state vector, $\mathbf{F}(k)$ is the system transition matrix, $\mathbf{G}(k)$ is the system noise input matrix and $\mathbf{w}(k)$ is the system noise vector which represents the instrument noise with any un-modelled errors with noise strength $\mathbf{Q}(k)$.

The continuous time SLAM/Inertial error model is based on misalignment angle dynamics and stationary feature model which is a random constant (Kim, 2004):

$$\begin{bmatrix} \delta \dot{\mathbf{p}}^n \\ \delta \dot{\mathbf{v}}^n \\ \delta \dot{\boldsymbol{\psi}}^n \\ \delta \dot{\mathbf{m}}_m^n \end{bmatrix} = \begin{bmatrix} \delta \mathbf{v}^n \\ \mathbf{C}_b^n \mathbf{f}^b \times \delta \boldsymbol{\psi}^n + \mathbf{C}_b^n \delta \mathbf{f}^b \\ -\mathbf{C}_b^n \delta \boldsymbol{\omega}^b \\ \mathbf{0}_m \end{bmatrix}, \quad (6)$$

where \mathbf{f}^b and $\boldsymbol{\omega}^b$ are acceleration and rotation rates measured from IMU, $\delta \mathbf{f}^b$ and $\delta \boldsymbol{\omega}^b$ are the associated errors in IMU measurement, \mathbf{C}_b^n is the direction cosine matrix formed from the quaternion. The discrete-time model can now be obtained by expanding the exponential state transition function and approximating it to the first-order term, and integrating the noise input during discrete sample time (Δt), which result in,

$$\mathbf{F}(k) = \begin{bmatrix} \mathbf{I} & \Delta t \mathbf{f}^n & \mathbf{0} & \mathbf{0} \\ \mathbf{0} & \mathbf{I} & \Delta t \mathbf{f}^n & \mathbf{0} \\ \mathbf{0} & \mathbf{0} & \mathbf{I} & \mathbf{0} \\ \mathbf{0} & \mathbf{0} & \mathbf{0} & \mathbf{I}_{m \times m} \end{bmatrix} \quad (7)$$

$$\mathbf{G}(k) = \begin{bmatrix} \mathbf{0} & \mathbf{0} \\ \sqrt{\Delta t} \mathbf{C}_b^n(k) & \mathbf{0} \\ \mathbf{0} & -\sqrt{\Delta t} \mathbf{C}_b^n(k) \\ \mathbf{0}_m & \mathbf{0}_m \end{bmatrix} \quad (8)$$

$$\mathbf{Q}(k) = \begin{bmatrix} \sigma_{\delta f}^2 & \mathbf{0} \\ \mathbf{0} & \sigma_{\delta \omega}^2 \end{bmatrix} \quad (9)$$

with $\sigma_{\delta f}$ and $\sigma_{\delta \omega}$ representing noise strengths of acceleration and rotation rate respectively.

3.3 Observation model

The linearised observation model can be obtained in terms of the observation residual, or measurement differences, $\delta \mathbf{z}(k)$ and the error states, $\delta \mathbf{x}(k)$,

$$\delta \mathbf{z}(k) = \mathbf{H}(k)\delta \mathbf{x}(k) + \mathbf{v}(k) \quad (10)$$

with $\mathbf{H}(k)$ being the linearised observation Jacobian and $\mathbf{v}(k)$ being the observation noise with noise strength matrix $\mathbf{R}(k)$. The error observations are generated by subtracting the measured quantity, $\tilde{\mathbf{z}}(k)$, from the INS predicted quantity $\hat{\mathbf{z}}(k)$,

$$\delta \mathbf{z}(k) = \delta \hat{\mathbf{z}}(k) - \delta \tilde{\mathbf{z}}(k). \quad (11)$$

As there are two different types of observation in this system, that is a range/bearing/elevation observation and a GNSS position/velocity observation, they should be formulated separately.

3.3.1 Range/Bearing/Elevation observation

In range/bearing/elevation observation, the onboard sensor provides relative observations between vehicle and features. The non-linear observation equation relates these observations to the state as

$$\mathbf{z}(k) = \mathbf{h}(\mathbf{x}(k), \mathbf{v}(k)), \quad (12)$$

where $\mathbf{h}(\cdot)$ is the non-linear observation model at time k , and $\mathbf{v}(k)$ is the observation noise vector. Since the

observation model predicts the range, bearing, and elevation for the i -th feature, it is only a function of the i -th feature and the vehicle state. Therefore Equation 8 can be further expressed as

$$\mathbf{z}_i(k) = \mathbf{h}(\mathbf{x}_v(k), \mathbf{x}_{mi}(k), \mathbf{v}_i(k)), \quad (13)$$

with $\mathbf{z}_i(k)$ and $\mathbf{v}_i(k)$ being the i -th observation and its associated additive noise in range, bearing and elevation with zero mean and variance of $\mathbf{R}(k)$. The feature position in the navigation frame is initialised from the sensor observation in the sensor frame and vehicle state as shown in Figure 3.

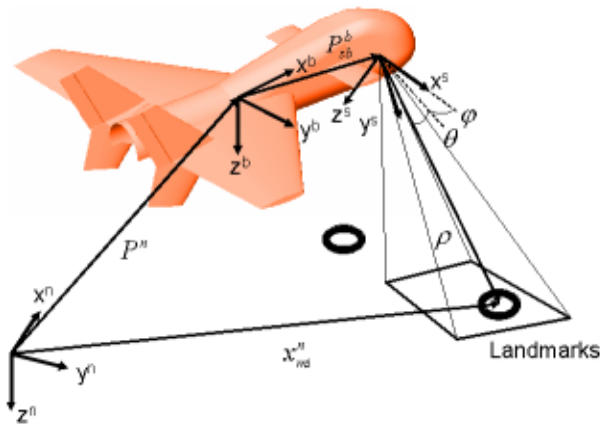


Fig. 3 The range, bearing and elevation observations from the onboard sensor can be related to the location of the feature in the navigation frame through the platform's position and attitude.

The initial feature position in the navigation frame is then computed

$$\mathbf{m}_i^n(k) = \mathbf{p}^n(k) + \mathbf{C}_b^n(k)\mathbf{p}_{bs}^b + \mathbf{C}_b^n(k)\mathbf{C}_s^b\mathbf{p}_{sm}^s(k) \quad (14)$$

where $\mathbf{p}_{bs}^b(k)$ is the lever-arm offset of the sensor from the vehicle's centre of gravity in the body frame, \mathbf{C}_s^b is a direction cosine matrix which transforms the vector in the sensor frame (such as camera instalment axes) to the body frame, and $\mathbf{p}_{sm}^s(k)$ is the relative position of the feature from the sensor expressed in the sensor frame which is computed from the observation:

$$\mathbf{p}_{sm}^s(k) = \begin{bmatrix} \rho \cos(\varphi) \cos(\vartheta) \\ \rho \sin(\varphi) \cos(\vartheta) \\ \rho \sin(\vartheta) \end{bmatrix}, \quad (15)$$

with ρ , φ and ϑ being the range, bearing and elevation angle respectively, measured from the onboard sensor. Hence the predicted range, bearing and elevation between

the vehicle and the i -th feature in Equation 8 can now be obtained by rearranging Equation 10,

$$\mathbf{z}_i(k) = \begin{bmatrix} \rho \\ \varphi \\ \vartheta \end{bmatrix} = \begin{bmatrix} \sqrt{x^2 + y^2 + z^2} \\ \tan^{-1}(y/x) \\ \tan^{-1}(z/\sqrt{x^2 + y^2}) \end{bmatrix}, \quad (16)$$

where,

$$\begin{bmatrix} x & y & z \end{bmatrix}^T = \mathbf{p}_{sm}^s(k) = \mathbf{C}_b^s \mathbf{C}_n^b(k) [\mathbf{m}_i^n(k) - \mathbf{p}^n(k) - \mathbf{C}_b^n(k) \mathbf{p}_{bs}^b] \quad (17)$$

The observation model is non-linear and has two composite functions; a coordinate transformation from the navigation frame to sensor frame, and transformation from Cartesian coordinates to polar coordinates. By calculating Jacobian of this equation, linearised discrete model is obtained:

$$\mathbf{H}(k) = \begin{bmatrix} \frac{\partial \rho}{\partial \mathbf{p}^n} & \frac{\partial \rho}{\partial \mathbf{v}^n} & \frac{\partial \rho}{\partial \Psi^n} \\ \frac{\partial \varphi}{\partial \mathbf{p}^n} & \frac{\partial \varphi}{\partial \mathbf{v}^n} & \frac{\partial \varphi}{\partial \Psi^n} \\ \frac{\partial \vartheta}{\partial \mathbf{p}^n} & \frac{\partial \vartheta}{\partial \mathbf{v}^n} & \frac{\partial \vartheta}{\partial \Psi^n} \end{bmatrix}, \mathbf{R}(k) = \begin{bmatrix} \sigma_\rho^2 & 0 & 0 \\ 0 & \sigma_\varphi^2 & 0 \\ 0 & 0 & \sigma_\vartheta^2 \end{bmatrix} \quad (18)$$

If vision or radar information is available, $\delta \mathbf{z}(k)$ is formed by subtracting the range, bearing and elevation of the sensor from the INS indicated range, bearing and elevation, then it is fed to the integrated fusion filter to estimate the errors in vehicle and map.

3.3.2 GNSS observation

GNSS can provide several observables such as position/velocity, pseudorange/pseudorange-rate, or integrated carrier phase. If the position/velocity observation is used the observation model simply becomes a linear form with,

$$\mathbf{H}(k) = \begin{bmatrix} \mathbf{I} & \mathbf{0} & \mathbf{0} & \mathbf{0}_m \\ \mathbf{0} & \mathbf{I} & \mathbf{0} & \mathbf{0}_m \end{bmatrix}, \mathbf{R}(k) = \begin{bmatrix} \sigma_p^2 & \mathbf{0} \\ \mathbf{0} & \sigma_v^2 \end{bmatrix}. \quad (19)$$

If GNSS information is available, $\delta \mathbf{z}(k)$ is formed by subtracting the position and velocity of the GNSS from the INS indicated position and velocity, then they are fed to the fusion filter to estimate the errors in vehicle and map.

3.4 K/F Prediction

With the state transition and observation models defined in Equations 6 and 9, the estimation procedure can proceed. The state and its covariance are predicted using the process noise input. The state covariance is propagated using the state transition model and process noise matrix by,

$$\delta \mathbf{x}(k|k-1) = \mathbf{F}(k)\delta \mathbf{x}(k-1|k-1) = \mathbf{0} \quad (20)$$

$$\mathbf{P}(k|k-1) = \mathbf{F}(k)\mathbf{P}(k-1|k-1)\mathbf{F}^T(k) + \mathbf{G}(k)\mathbf{Q}(k)\mathbf{G}^T(k)$$

Not only is the linear prediction much simpler and computationally more efficient than in the direct SLAM approach, but furthermore the predicted error estimate, $\delta \mathbf{x}(k|k-1)$, is zero. This is because if one assumes that the only error in the vehicle and map states is zero mean Gaussian noise, then there is no error to propagate in the state prediction cycle, and the uncertainty in this assumption is provided in the covariance matrix propagation.

3.5 K/F Estimation

When an observation occurs, the state vector and its covariance are updated according to

$$\delta \mathbf{x}(k|k) = \delta \mathbf{x}(k|k-1) + \mathbf{W}(k)\mathbf{v}(k) = \mathbf{W}(k)\mathbf{v}(k) \quad (21)$$

$$\mathbf{P}(k|k) = \mathbf{P}(k|k-1) - \mathbf{W}(k)\mathbf{S}(k)\mathbf{W}^T(k). \quad (22)$$

where the innovation vector, Kalman weight, and innovation covariance are computed as,

$$\mathbf{v}(k) = \mathbf{z}(k) - \mathbf{H}(k)\delta \mathbf{x}(k|k-1) = \mathbf{z}(k) \quad (23)$$

$$\mathbf{W}(k) = \mathbf{P}(k|k-1)\mathbf{H}^T(k)\mathbf{S}^{-1}(k) \quad (24)$$

$$\mathbf{S}(k) = \mathbf{H}(k)\mathbf{P}(k|k-1)\mathbf{H}^T(k) + \mathbf{R}(k), \quad (25)$$

where, for the same reason as in the prediction cycle, $\mathbf{H}(k)\delta \mathbf{x}(k|k-1)$ is zero and hence is not explicitly computed.

3.6 Feedback Error Correction

Once the observation estimation has been processed successfully, the estimated errors are now fed to the external INS loop and the map for correction. The corrected position, $\mathbf{p}_c^n(k)$, and velocity, $\mathbf{v}_c^n(k)$, are obtained by subtracting the estimated errors, and The corrected attitude quaternion, $\mathbf{q}_c^n(k)$, is obtained by pre-multiplying the error quaternion to the current quaternion:

$$\mathbf{p}_c^n(k) = \mathbf{p}^n(k) - \delta \mathbf{p}^n(k|k) \quad (26)$$

$$\mathbf{v}_c^n(k) = \mathbf{v}^n(k) - \delta \mathbf{v}^n(k|k) \quad (27)$$

$$\mathbf{q}_c^n(k) = \delta \mathbf{q}^n(k) \otimes \mathbf{q}^n(k), \quad (28)$$

where the error quaternion $\delta \mathbf{q}_c^n(k)$ is computed from the estimated misalignment angle:

$$\delta \mathbf{q}^n(k) \cong \left[1 \quad \delta \psi_x/2 \quad \delta \psi_y/2 \quad \delta \psi_z/2 \right]^T. \quad (29)$$

The corrected map positions are directly obtained by subtracting the estimated map position errors from the current positions:

$$(\mathbf{m}_N^n)_c(k) = \mathbf{m}_N^n(k) - \delta \mathbf{m}_N^n(k|k). \quad (30)$$

Using these equations the complementary SLAM/GNSS/INS Kalman filter can recursively fulfil its cycle of prediction and estimation with the external INS loop and the map.

3.6. Data Association and Feature Augmentation

Data association is a process that finds out the correspondence between observations at time k and features registered. Correct correspondence of the sensed feature observations to mapped features is essential for consistent map construction, and a single false match can invalidate the entire SLAM estimation process. Association validation is performed in observation space. As a statistical validation gate, the Normalised Innovation Square (NIS) is used to associate observations. The NIS (γ) is computed by

$$\gamma = \mathbf{v}^T(k)\mathbf{S}^{-1}(k)\mathbf{v}(k). \quad (31)$$

Given an innovation and its covariance with the assumption of Gaussian distribution, γ forms a χ^2 (chi-square) distribution. If γ is less than a predefined threshold, then the observation and the feature that were used to form the innovation are associated. The threshold value is obtained from the standard χ^2 tables and is chosen based on the confidence level required. Thus for example, a 99.5% confidence level, and for a state vector which includes three states of range, bearing, and elevation, then the threshold is 12.8. The associated innovation is now used to update the state and covariance. If the feature is re-observed then the estimation cycle proceeds, otherwise it is a new feature and must be augmented into both the external map and the covariance matrix (Kim, 2004).

4. Results

A simulation analysis is performed to verify the proposed algorithm for the Brumby UAV, developed in University of Sydney, under GNSS enabled and disabled scenarios.

4.1 Simulation Environment

A low-cost IMU is simulated with a vision as the range, bearing, and elevation sensor. The vision sensor used in the real system provides range information based on knowledge of target size; hence its range is simulated with large uncertainty. The simulation parameters obtained from the implemented actual sensor specifications are listed in Table I.

Table 1. The parameters used in simulation

Sensor	Specification	Parameter
IMU	Sampling rate (Hz)	50
	Accel noise ($m/s^2/\sqrt{Hz}$)	0.5
	Gyro noise ($^\circ/s/\sqrt{Hz}$)	0.5
Vision	Frame rate (Hz)	25
	Field-Of-View ($^\circ$)	± 15
	Estimated range error (m)	≥ 5
	Bearing noise ($^\circ$)	0.16
	Elevation noise ($^\circ$)	0.12
GNSS	Position noise (m)	2.0
	Velocity noise (m/s)	0.5

The flight vehicle undergoes three race-horse trajectories approximately 100m above the ground. The flight time is 460 seconds and the average flight speed is 40m/s. There are 80 features placed on the ground. The vision observation is expressed in a camera frame, which is transformed to navigation frame to be processed in the SLAM node. The biases of the IMU are calibrated precisely using onboard inclinometers in the real implementation thus the biases are not explicitly modelled and studied in the simulation analysis and only white noise is modelled as in Table 1.

4.2 GNSS Active Region: Map Building

Figure 4 shows the SLAM/GNSS/INS estimated vehicle trajectory with the map built during the flight. The map uncertainty ellipsoids are also plotted with 10σ boundaries for the clarification. The vehicle takes off and flies over circuit-1 two rounds. It then transits to circuit-2 and circuit-3. To simulate GNSS denied scenario, GNSS signal is disabled between 130 to 420 seconds from the start. After the vehicle taking off, GNSS signal is available until 130 seconds. The system behaves as a

feature-tracking/mapping system in this mode. The error covariance of features around circuit-1 has relatively small value than features around other circuits. Figure 9 presents the evolution of uncertainties of the vehicle and map. It can be clearly observed that the vehicle uncertainty was maintained within one metre until 130 seconds, and the uncertainties of observed features are monotonically decreased. INS error is dominantly estimated from GNSS information, and the GNSS/INS blended navigation solution is used to track features. Contrary to the conventional airborne mapping systems, SLAM/GNSS/INS system maintains the cross-correlation information between the INS and map which can enhance the INS performance, and it is essential for the SLAM operation in GNSS denied conditions.

4.3 GNSS Denied Region: SLAM/INS navigation

In this condition, the SLAM/GNSS/INS system now behaves as a SLAM/INS system. INS and map errors are solely estimated from the feature observation. The pre-registered feature during GNSS active period can be effectively used to estimate the INS and map errors as shown in Figures 5 to 8. After GNSS is disabled, INS uncertainties begin to increase which in turn increases the registered map uncertainties. The accumulated INS error is effectively removed from the closing-the-loop effect, which, in turn, eliminates the INS error embodied in the map. This can be observed in INS and map covariance plot as in Figure 13. Figures 10 and 11 show the evolution of uncertainty of INS velocity and attitude which are constrained effectively for extended period of time without GNSS aiding. This is due to the correlation structure between vehicle and the map in SLAM. The map uncertainty decreases monotonically and whenever the vehicle observes the feature, the vehicle error can be constrained effectively until GNSS signal is available again. Figures 12 shows the final map uncertainties built in GNSS enabled and disabled conditions. When GNSS signal is re-activated, the INS position and velocity errors are directly observed from the GNSS measurements, which, in-turn, improves the map accuracy via the vehicle-map correlation structure within SLAM filter. From these plots, it is obvious that the SLAM/GNSS/INS system can perform navigation and mapping for extended periods of time under GNSS denied conditions.

5 Conclusions

A new concept for UAV navigation is presented based on 6DoF Simultaneous Localisation and Mapping (SLAM) algorithm, and augmenting it to GNSS/INS system. The simulation analysis illustrates that the SLAM system with a range, bearing, and elevation sensor can constraint the INS errors effectively, performing on-line map building

in GNSS denied and unknown terrain environments for extended periods of time. It can be applied to various navigation areas such as battlefield situations, urban canyons, indoor, or underwater. The real-time implementation on UAV platform using low-cost sensor are being tackled at the moment.

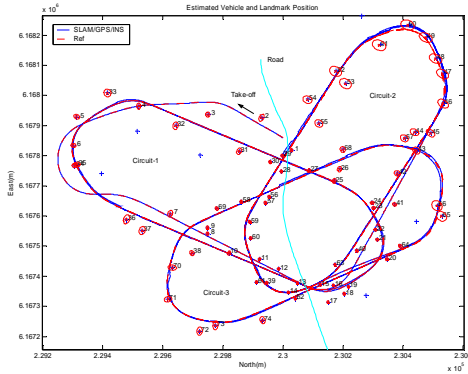


Figure 3. 2D position result of the SLAM augmented GNSS/INS navigation. UAV takes off at (0,0) and flies three different race-horse tracks (circuit-1,2,3) in counter clock-wise. GNSS signal is disabled in circuit-1 and re-enabled at the end of in circuit-3. The vision is available during whole flight time which is used for feature-mapping and SLAM.

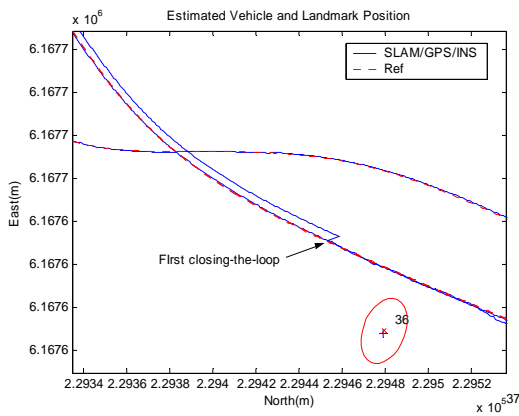


Figure 4. Enhanced view of INS correction by the closing-the-loop effect of SLAM during GNSS disabled condition.

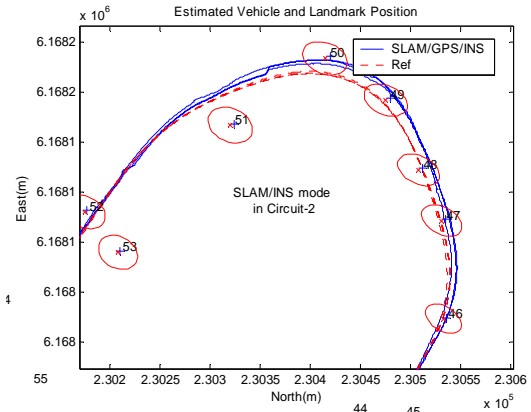


Figure 5. SLAM incrementally builds new map during GNSS disabled condition.

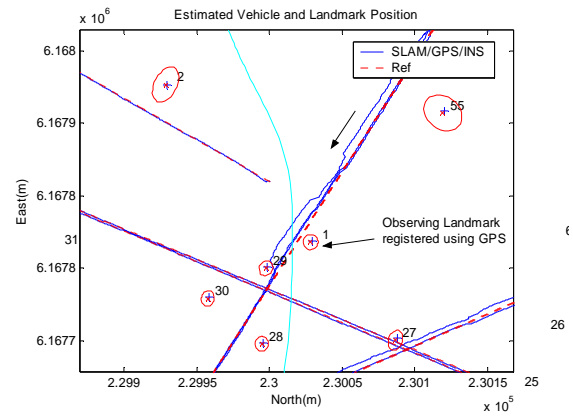


Figure 6. Enhanced view of INS correction by re-observing previously built map by GNSS.

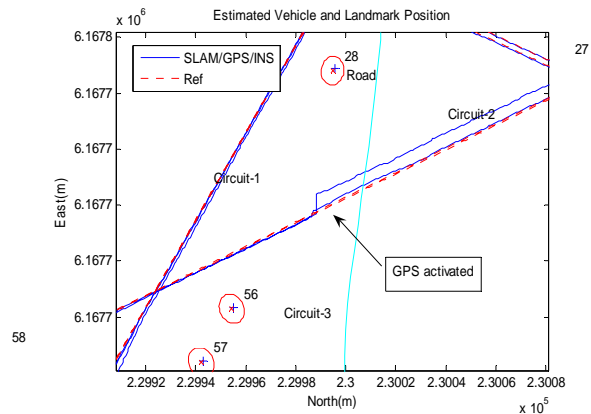


Figure 7. GNSS is re-enabled and it corrects both INS and map error simultaneously.

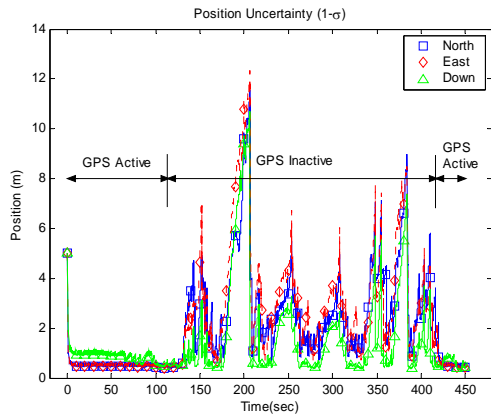


Figure 8. Evolution of INS position uncertainty during flight. It can be observed that SLAM can bound the error growth during GNSS denied condition for extended period of time. GNSS is disabled at 130 second and re-enabled at 420 second

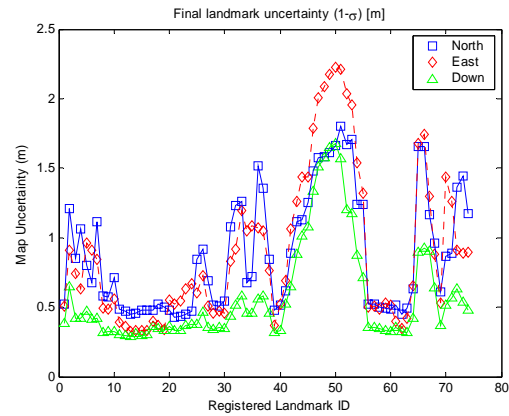


Figure 11. Final map uncertainty. The features registered during GNSS denied condition show larger uncertainties due to the accumulated INS error.

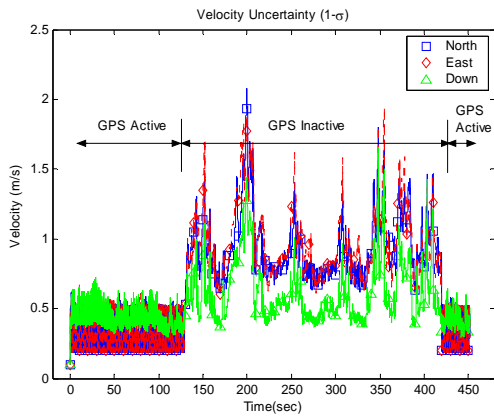


Figure 9. Evolution of INS velocity uncertainty during flight.

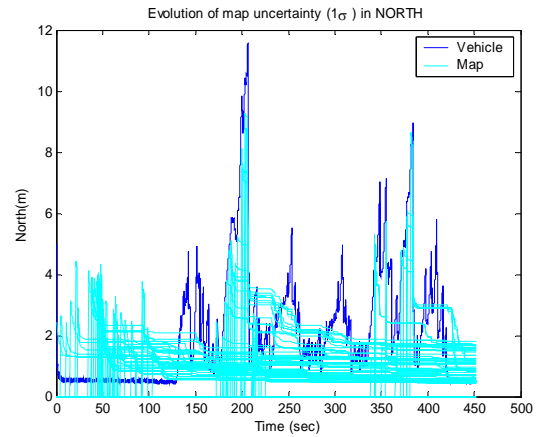


Figure 12. Evolution of INS position and map uncertainties in north direction. The map uncertainty converges to the lower limit monotonically.

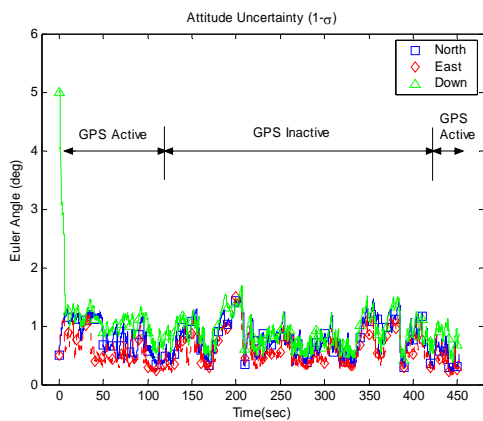


Figure 10. Evolution of INS attitude uncertainty during flight.

Acknowledgements

This work is supported in part by the ARC Centre of Excellence programme, funded by the Australian Research Council (ARC) and the New South Wales State Government.

References

Dissanayake M.W.M.G.; Newman P.; Durrant-Whyte H.; Clark S.; Csorba M. (2001): *A solution to the simultaneous localization and map building problem*, IEEE Transactions on Robotics and Automation, June, 17(3):229–241.

Guivant J.; Nebot E. (2001): *Optimisations of the simultaneous localization and map building algorithm for real-time*

- implementation*, IEEE Transactions on Robotics and Automation, 17(3):242–257.
- Kim J.; Sukkariah S. (2004): *Autonomous Airborne Navigation in Unknown Terrain Environments*, IEEE Transactions on Aerospace and Electronic Systems, 40(3):1031-1045, July
- Kim J. (2004): *Autonomous Navigation for Airborne Applications*, PhD thesis, Australian Centre for Field Robotics, The University of Sydney.
- Smith R.; Cheeseman P. (1987) *On the Representation of Spatial Uncertainty*, In International Journal of Robotics Research, 5(4):56–68.
- Williams S.B.; Dissanayake M.W.M.G.; Durrant-Whyte H. (2001): *Towards terrain-aided navigation for underwater robotics*, In Advanced Robotics, 15(5):533–550.